Experimental Comparison of Conventional PID, Adaptive PID, and Hysteresis Temperature Control in a Laboratory-Scale Vegetable-Oil Biodiesel Reactor

Nikolaus Dharmawan Dharsono
Department of Electrical Engineering, Faculty of Applied Science and Technology, Institut Sains dan Teknologi Nasional, Jakarta, Indonesia

Lilly S. Wasitova
Department of Electrical Engineering, Faculty of Applied Science and Technology, Institut Sains dan Teknologi Nasional, Jakarta, Indonesia

Masbah R.T. Siregar
Department of Electrical Engineering, Faculty of Applied Science and Technology, Institut Sains dan Teknologi Nasional, Jakarta, Indonesia

Abstract: The increasing demand for energy and the limited availability of diesel fuel have encouraged the development of biodiesel as a renewable energy source. Temperature stability during transesterification is important because it affects reaction performance and biodiesel yield. This study aimed to experimentally compare conventional PID, adaptive PID, and hysteresis temperature control in a laboratory-scale biodiesel reactor. The system was tested using palm oil and castor oil at setpoints of 50°C and 60°C with conventional PID, adaptive PID, and hysteresis control. Each combination of control method, feedstock, and temperature was evaluated in a single experimental run. The system consisted of a Type-K thermocouple, temperature controller, solid-state relay, heating element, magnetic stirrer, RS-485 module, and computer. Performance was evaluated based on rise time, overshoot, settling time, steady-state error, density, and yield. Under the tested conditions, adaptive PID produced no overshoot and showed the lowest observed controller-indicated steady-state error of 0.056°C. Hysteresis control produced the shortest rise and settling times but showed the highest observed steady-state error of 0.625°C and overshoot under several conditions. The highest observed yield in the single-run experiments was 95.423%, obtained from castor oil at 60°C using adaptive PID.

Keywords: Biodiesel, hysteresis, PID, adaptive PID, yield.

Correspondents Author:
Nikolaus Dharmawan Dharsono, Department of Electrical Engineering, Faculty of Applied Science and Technology, Institut Sains dan Teknologi Nasional, Jakarta, Indonesia
Email: nikolauz.dd@gmail.com

Received July 24, 2025; Revised July 31, 2026; Accepted August 1, 2026; Published August 4, 2026.

Introduction

The continuing growth of global energy demand, the finite availability of fossil-fuel resources, and concerns regarding greenhouse-gas emissions have intensified the search for renewable transportation fuels. Biodiesel has emerged as a renewable and sustainable alternative to petroleum-based fuels (Mhetras & Gokhale., 2025). It can be produced from various renewable lipid feedstocks, including edible and non-edible vegetable oils, thereby offering an alternative pathway for reducing dependence on fossil-based fuels (Naseef & Tulimat, 2025). Biodiesel is generally produced through transesterification, in which triglycerides contained in vegetable oil react with an alcohol in the presence of a catalyst to form fatty-acid alkyl esters and glycerol (Naseef & Tulimat, 2025; Haryono et al., 2025). The effectiveness of this reaction is influenced by the alcohol-to-oil ratio, catalyst concentration, mixing conditions, reaction duration, feedstock properties, and reaction temperature. Among these variables, temperature requires particular attention because it affects reaction kinetics, mixture viscosity, mass-transfer behavior, and methanol evaporation. An insufficient temperature may reduce the reaction rate, whereas an excessive or unstable temperature may increase methanol loss and promote undesirable reactions, thereby affecting the amount of recovered biodiesel. An appropriate temperature-control system is therefore required to bring the reactor temperature to the intended setpoint and maintain it during the transesterification process. In laboratory- and pilot-scale biodiesel systems, conventional PID control has commonly been applied because of its simple structure and compatibility with commercial process controllers. (Fong and Abu Bakar .,2023), for example, evaluated PID tuning for the heating process of a biodiesel pilot plant using fixed controller parameters selected through trial-and-error testing. Another experimental study compared PD, PI, and PID operating modes in a biodiesel pilot-plant vessel and selected fixed PID parameters based on overshoot and rise time (Musa., 2023). These studies demonstrated the practical applicability of PID control, but the selected parameters remained unchanged during operation and were obtained for particular plant conditions. Consequently, the controller could not automatically compensate for changes in the process response caused by different feedstocks and setpoints. Simple temperature-regulation systems may also employ ON/OFF control, in which the heater is switched according to the difference between the process temperature and the setpoint. The addition of a hysteresis band can reduce repeated switching around a single threshold and makes this method relatively easy to implement using a commercial temperature controller. However, ON/OFF hysteresis control does not continuously regulate the heater output and may produce cyclic temperature fluctuations or overshoot because heating energy remains in the system after the heater is switched off. Although this approach is suitable for low-cost thermal systems, its response-speed advantage must therefore be considered together with its potential limitations in steady-state temperature stability. More advanced control approaches have been proposed to overcome the limitations of fixed PID and ON/OFF control. (Çağatay and Karacan., 2022) experimentally compared discrete-time PID with nonlinear generalized predictive control for temperature regulation in a reactive-distillation biodiesel process. (Martínez-Sánchez et al.,2022 ; Manimaran et al., 2023 ; Patti et al., 2024) investigated plantwide, model-predictive, and hierarchical control structures for continuous biodiesel production. (Maya-Rodriguez et al., 2023) also developed a neuro-fuzzy temperature controller optimized using a metaheuristic technique to improve biodiesel-reactor performance. These approaches offer advantages in handling multivariable interactions, disturbances, and nonlinear process behavior. However, these approaches generally require process models, system identification, optimization procedures, and multiple computational stages, which can increase implementation complexity and development time. Therefore, more practical control alternatives are needed. Adaptive PID can modify its controller parameters according to the observed temperature response, while hysteresis control can adjust its switching band based on the process behavior. Both approaches can be implemented without requiring a complete process model or extensive optimization procedures. Adaptive PID control has also been investigated in several process-control applications because of its ability to adjust controller parameters in response to changes in system behavior. (Adriansyah et al., 2025), for example, applied an adaptive PID strategy in a dynamic control system, while (Yulianto et al., 2023) discussed the development of adaptive and predictive control for thermal and pressure regulation. These studies demonstrate that parameter adaptation can improve controller flexibility under changing operating conditions. However, the reported applications were not focused on batch biodiesel transesterification and did not examine the online adjustment of PID parameters in a commercial temperature controller using the measured temperature response as supervisory information. In addition, the direct experimental relationship between dynamic temperature-control performance and recovered biodiesel yield was not explicitly evaluated in the reviewed studies. Recent studies have demonstrated the potential of large language models (LLMs) as supervisory components in adaptive control systems.(Zahedifar et al., 2025) showed that an LLM-based controller could adapt a robot-control strategy in response to changes in system dynamics, reference signals, disturbances, and unmodeled behavior. More specifically, (Arif and Rahim., 2025) experimentally implemented LLM agents for real-time PID tuning in a servo-motor system, where the agents monitored performance indicators and updated PID parameters within predefined safe limits, resulting in reductions in several control-error metrics. A recent process-control study also reported that an LLM-assisted supervisory PID architecture improved the response of a nonlinear water-tank system, whereas direct LLM control alone was unable to achieve stable regulation, supporting the use of LLMs as supervisory tuners rather than replacements for deterministic feedback controllers (Wen et al., 2026). Based on these findings, the present study employed Llama 3.1 8B Instruct as the supervisory model because its 8-billion-parameter size was considered suitable for local execution with lower computational requirements than larger LLMs, while retaining instruction-following capability for processing structured temperature-response information. The model was therefore used only to generate bounded parameter-adjustment decisions, while the commercial controller remained responsible for real-time PID calculation and heater switching. Palm oil and castor oil were selected as the feedstocks because they represent vegetable oils with different practical and physicochemical characteristics. Palm oil is widely available and commonly used as a biodiesel feedstock, particularly in tropical countries, whereas castor oil is a non-edible feedstock with a distinctive fatty-acid composition and relatively high viscosity (Angassa et al., 2023; Naseef & Tulimat, 2025). These differences may affect heat transfer, mixing behavior, and the temperature response during transesterification. Evaluating both feedstocks therefore provides a practical basis for examining whether the control system can maintain its performance under different process conditions. However, this study does not attempt to determine the intrinsic effects of feedstock properties because viscosity, heat capacity, and fatty-acid composition were not independently characterized.

Based on the reviewed studies, a research gap remains in the experimental implementation of fixed PID, adaptive PID, and hysteresis control using the same laboratory-scale biodiesel reactor, commercial temperature controller, sensor, actuator, initial parameter baseline, feedstocks, and temperature setpoints. Previous studies have generally evaluated individual control methods, applied advanced model-based strategies, or focused on continuous production systems. Limited attention has been given to a practical supervisory architecture in which PID parameters and the hysteresis band are adjusted according to the observed temperature response without requiring a complete mathematical process model. To address this gap, the present study proposes a response-based supervisory control approach in which an LLM-assisted supervisory layer evaluates the measured temperature behavior and generates bounded adjustments to the PID parameters and hysteresis band. The supervisory mechanism considers indicators such as temperature rate of change, proximity to the setpoint, overshoot, and steady-state error. LLMs have shown potential as supervisory components for interpreting process information and supporting controller-parameter adjustment while conventional controllers continue to perform deterministic real-time control. In this study, Llama 3.1 8B Instruct was selected because its instruction-tuned architecture and relatively compact 8-billion-parameter size were considered suitable for local execution and structured decision-making. The model was used only for supervisory parameter-adjustment decisions and did not directly calculate the control output or switch the heater. Therefore, the novelty of this study lies not only in comparing three temperature-control methods, but also in implementing a locally executed, response-based supervisory mechanism that adjusts controller parameters according to the observed process behavior without requiring a complete mathematical process model or extensive optimization procedures. Accordingly, this study aims to experimentally compare conventional PID, adaptive PID, and hysteresis temperature control in a laboratory-scale biodiesel reactor using palm oil and castor oil at setpoints of 50 °C and 60 °C. The study provides descriptive experimental information on how the adaptive PID system responds to changes in feedstock and temperature setpoint compared with conventional PID and hysteresis control under the tested conditions. The use of the same reactor hardware and common initial PID baseline provides a consistent basis for the comparison. The observed results may serve as an initial reference for future studies involving replicated experiments and larger reactor capacities.

Research Method

Materials and Instruments

The materials and instruments used in this study are presented in Table 1 and Table 2. The experimental system was a custom-built laboratory-scale setup based on the general configuration of a stirred-tank reactor, consisting of a reactor vessel, heating system, and mixing system. A 1000 mL borosilicate measuring cylinder was used as the reactor vessel, with an approximate total working volume of 900 mL per batch, including vegetable oil, methanol at a methanol-to-oil molar ratio of 9:1, and NaOH catalyst at 1% (w/w) of the oil mass. A magnetic stirrer provided continuous mixing, while a 350 W electrical heating element supplied heat to the reaction mixture. Temperature measurement and regulation were performed using a Type-K thermocouple, an Autonics TK4S temperature controller, and a Fotek 40DA solid-state relay. The system was therefore configured as a custom-built laboratory-scale stirred reactor equipped with temperature-control and monitoring components. The effective thermal capacity, thermal inertia, process time constant, and dead time were not independently characterized in the original experimental design.

Table 1 Biodiesel Research Material

Classification	Material
Reactants	Sodium hydroxide (NaOH) Industrial-grade methanol
Main feedstocks	Sunflower seed oil (CXS, 1999) Castor oil (Ricinus communis) (SNI, 1990) Palm oil (SNI, 2019)
Supporting material	Distilled water

The research materials were classified into three groups: reactants, main feedstocks, and supporting materials. Reactants are chemical substances involved in the transesterification reaction, consisting of industrial-grade methanol and sodium hydroxide as the catalyst. The main feedstocks are vegetable oils used as the primary source of triglycerides, including sunflower seed oil, castor oil, and palm oil. Distilled water was used as a supporting material during the biodiesel washing process. During transesterification, the borosilicate measuring-cylinder reactor was covered with plastic wrap to limit direct vapor release. The vessel was not hermetically sealed, was not operated under pressure, and was not equipped with a reflux condenser.

Table 2 Biodiesel Research Instrument

Classification	Instrument
Process equipment	1000 mL measuring cylinder 350 W heating element
Control equipment	Magnetic stirrer Type-K thermocouple temperature sensor with an accuracy of ±0.4% of the measured value (ASTM, 2024) Fotek 40DA solid-state relay Autonics TK4S
Supporting equipment	Computer 1000 mL separating funnel RS-485
Software	Python 3.11 Visual Studio Code 1.129.1 Llama 3.1 8B Instruct

The research instruments were classified into four groups: reactor and process equipment, control and instrumentation equipment, supporting equipment, and software. The reactor and process equipment represented the main components of a laboratory-scale stirred reactor. The measuring cylinder served as the reactor vessel, the heating element supplied thermal energy, and the magnetic stirrer maintained uniform mixing of the reactants. The control and instrumentation equipment was used to measure, regulate, and monitor the reactor temperature. The Type-K thermocouple measured the process temperature, the Autonics TK4S processed the temperature signal and generated the control command, and the Fotek 40DA solid-state relay regulated the electrical power supplied to the heating element. The RS-485 interface enabled communication between the temperature controller and the computer. Supporting equipment was used for system operation and product separation, while the software was used for control supervision, data acquisition, and processing.

Temperature Control System Component Configuration

The design of the research equipment used for biodiesel production in this study is presented in Figure 1.

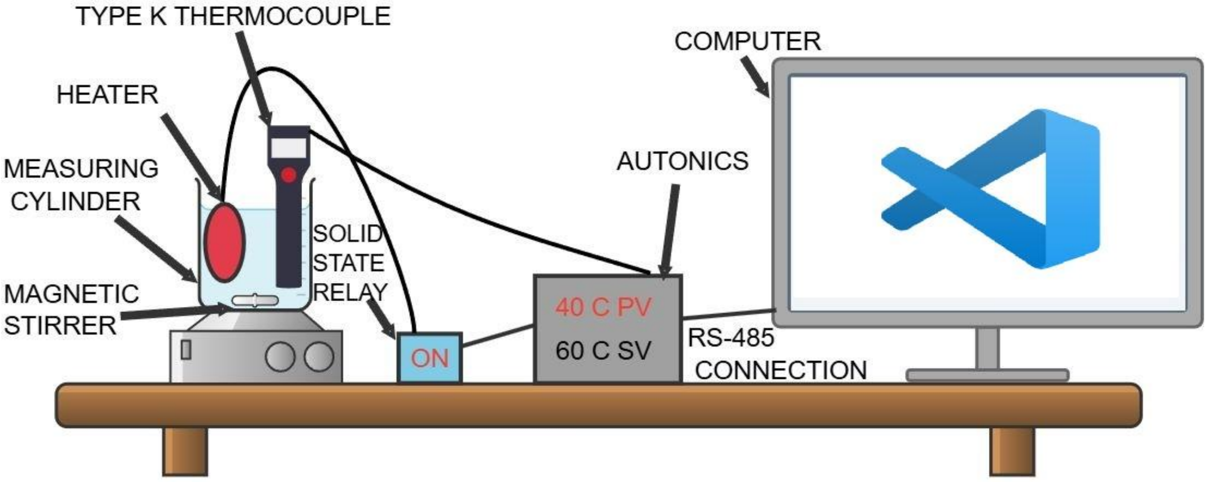

Figure 1 Design of the Biodiesel Research Reactor

Based on Figure 1, the research setup consisted of a measuring cylinder as the biodiesel reactor, a magnetic stirrer, a heating element, a Type-K thermocouple, a solid-state relay (SSR), an Autonics temperature controller, an RS-485 communication module, and a computer. The measuring cylinder was used as the transesterification vessel, while the magnetic stirrer was used for the stirring process. The heating element served as the heat source, and the Type-K thermocouple was used to measure the actual reaction temperature. The temperature data were received by the Autonics controller and compared with the setpoint values. The RS-485 communication module was used to connect the Autonics controller to the computer, enabling temperature monitoring, data logging, and control parameter communication during the experiment. The computer was used for temperature monitoring, data logging, and supervisory support during the experiment. The interconnection diagram of the temperature control system components is presented in Figure 2.

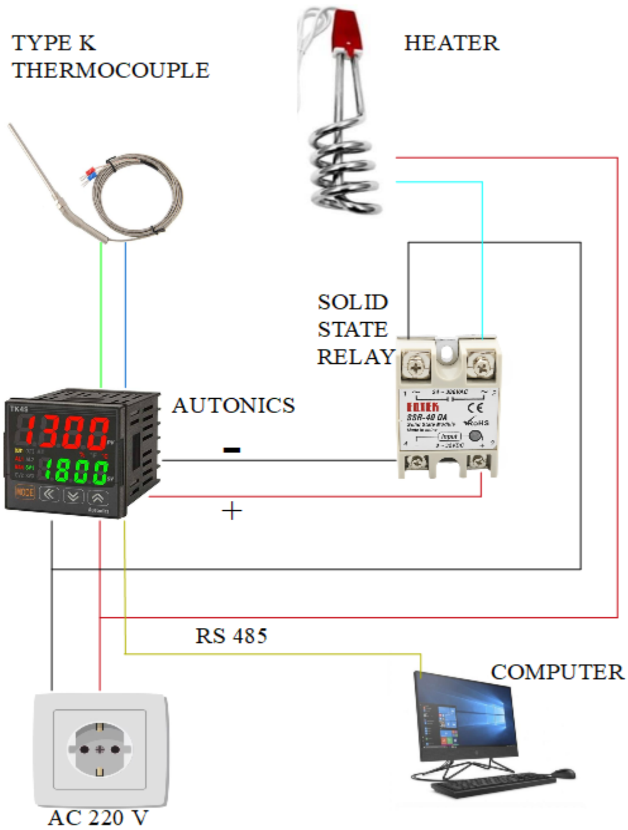

Figure 2 Interconnection Diagram of the PID, Adaptive PID, and Hysteresis Control System Components

The system consisted of a Type-K thermocouple as the temperature sensor, an Autonics temperature controller as the main controller, a solid-state relay (SSR) as the electronic switch, a heating element as the actuator, an RS-485 communication module as the interface between the controller and the computer, a computer for monitoring and data logging, and a 220 V AC power source. The thermocouple measured the actual temperature during the heating process and sent the signal to the Autonics controller. The Autonics TK4S served as the main controller in which the conventional PID, adaptive PID, and ON/OFF hysteresis control methods were implemented. The control parameters, including the proportional, integral, and derivative parameters for PID control and the hysteresis value for ON/OFF control, were applied and stored in the Autonics controller. Based on the measured temperature and the selected control parameters, the controller generated an output command to the SSR. The SSR then connected or disconnected the electrical current supplied to the heating element according to the command from the Autonics controller. The computer was connected to the Autonics TK4S controller through RS-485 communication for process-temperature monitoring, data logging, and supervisory parameter adjustment. The Autonics TK4S, as a commercial controller, provided the built-in autotuning function, real-time PID calculation, ON/OFF hysteresis operation, and output switching of the solid-state relay. In conventional PID control, the PID parameters obtained from the Autonics autotuning process were stored in the controller and remained fixed throughout the experiment. In adaptive PID control, the Autonics TK4S continued to execute its built-in PID algorithm, while an external supervisory module developed by the authors evaluated the measured temperature response and transmitted updated PID parameter values through RS-485 communication. The external supervisory system consisted of a Python 3.11 application and a locally executed Llama 3.1 8B Instruct model. Python handled data acquisition, communication with the Autonics controller, parameter-limit checking, and transmission of updated PID values. The supervisory decision logic evaluated the temperature rate of change, proximity to the setpoint, overshoot, and steady-state error before recommending bounded adjustments to the P, I, and D parameters. In ON/OFF hysteresis control, the Autonics TK4S independently switched the heating element according to the upper and lower temperature limits defined by the stored hysteresis parameter. Therefore, the commercial controller provided the real-time control and actuator-switching functions, whereas the authors' original contribution consisted of the external supervisory software, response-evaluation logic, bounded PID-parameter adjustment mechanism, and RS-485 communication procedure. Therefore, the three control methods used the same basic hardware configuration. Their main differences were the control mode, the source of the control parameters, and the parameter-adjustment mechanism. Conventional PID used fixed parameters, adaptive PID used externally updated parameters generated by the supervisory module, and ON/OFF hysteresis used the hysteresis setting stored in the Autonics controller.

Experimental Design and Procedure

The experimental design was established to assess the temperature control performance of the proposed supervisory adaptive PID strategy and to compare it with the conventional hysteresis control method under the same operating conditions. All experiments were conducted in the same biodiesel reactor, heating element, temperature sensor, controller configuration, and operating parameters to ensure a fair comparison. The dynamic response of the control system was analyzed in terms of rise time, overshoot, settling time, steady-state error and temperature stability during the transesterification process by continuously always recording temperature data during each experiment.

The full sequence of the experimental procedure is shown in Figure 3. The procedure begins with system initialization and sensor calibration, and then the biodiesel reactor is prepared and the heating and mixing systems are activated. During the experiment the controller continuously measures the temperature and based on the selected control strategy it adjusts the heating process. After the reactor reaches the desired operating temperature, the temperature response is recorded for the duration of the reaction, and the data is analyzed to assess the effectiveness, stability and control performance of the proposed method.

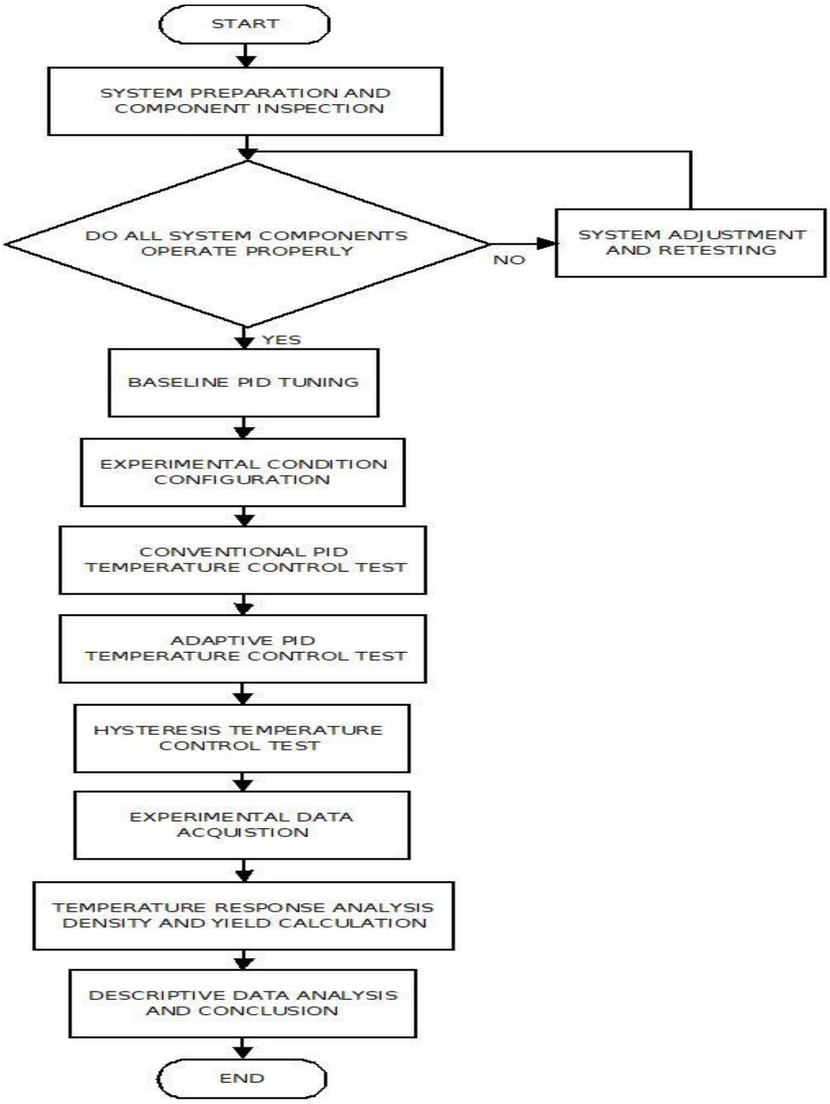

Figure 3 Overall Workflow of the Experimental Procedure

Figure 3 presents the experimental workflow used in this study. The procedure began with the preparation of the biodiesel reactor, temperature-control equipment, measurement devices, and communication system, followed by an inspection to ensure that all components operated properly. If a malfunction or communication problem was identified, the system was adjusted and retested before the experiment continued. After the system had passed the functional inspection, baseline PID tuning was conducted to determine the initial controller parameters used as a common reference for the conventional and adaptive PID experiments. The experimental conditions were then configured according to the predetermined combinations of control method, vegetable-oil feedstock, and temperature setpoint. Conventional PID, adaptive PID, and hysteresis temperature-control tests were conducted separately during the biodiesel transesterification process. Throughout each experimental run, the reactor temperature was recorded for the evaluation of rise time, overshoot, settling time, and steady-state error. After the transesterification and product-purification stages were completed, the recovered biodiesel was evaluated through density measurement and yield calculation. The resulting temperature-response and biodiesel data were subsequently analyzed descriptively to compare the observed performance of the three control methods under the tested conditions and to formulate the conclusions of the study.

The laboratory-scale biodiesel reactor and temperature control system used in this study are shown in Figure 4. The system represents the implemented hardware configuration of the laboratory-scale biodiesel reactor and temperature control system. It consisted of an Autonics TK4S temperature controller, a solid-state relay, a 350 W heating element, a magnetic stirrer, a Type-K thermocouple, an RS-485 communication interface, and a computer for monitoring, data logging, and supervisory control.

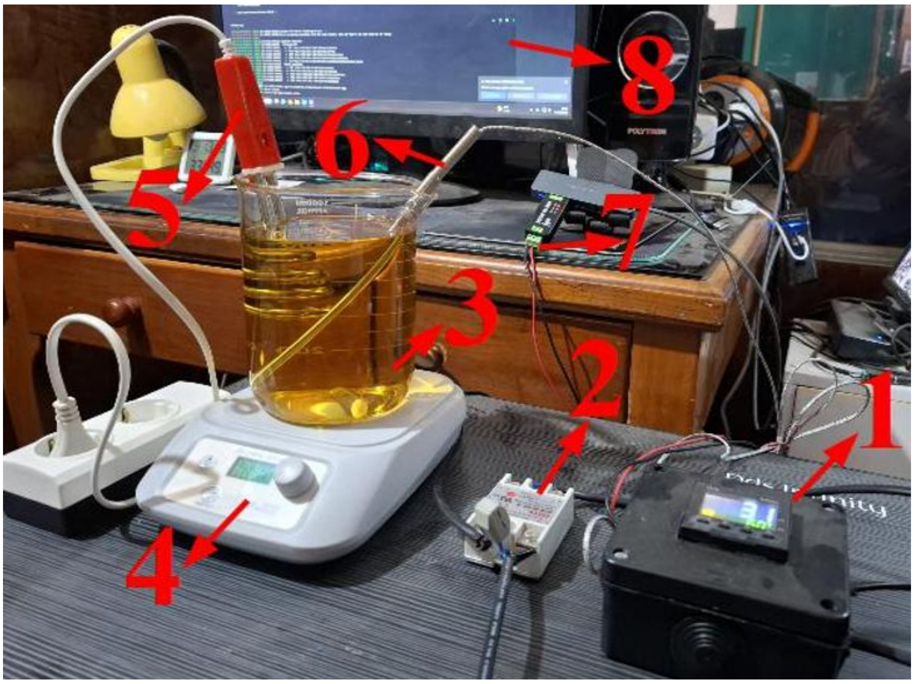

Figure 4 Laboratory-scale biodiesel reactor and temperature control system

Figure 4 shows the laboratory-scale biodiesel reactor and temperature-control system used in this study. The system consisted of an Autonics TK4S temperature controller (1), a solid-state relay (2), a 1000 mL measuring cylinder used as the reactor vessel (3), a magnetic stirrer (4), a heating element (5), a Type-K thermocouple (6), an RS-485 communication module (7), and a computer (8). The reactor had a working capacity of 900 mL per batch. During the reaction process, the magnetic stirrer was operated at a nominal setting of 600 rpm to mix the reaction mixture, while the heating element supplied heat. The stirrer model was M-SCL-T 2000 mL, and a magnetic stir bar with dimensions of 3 cm was used. The rotational speed was set using the stirrer control and was not independently verified using an external tachometer. Uniform mixing was assessed only through visual observation of continuous circulation of the reaction mixture; no quantitative mixing-time, velocity-field, or homogeneity test was performed for the different vegetable oils. Therefore, differences in viscosity may have affected the mixing behavior, although this effect was not independently evaluated in the present study.

The Type-K thermocouple measured the process temperature and transmitted the signal to the Autonics TK4S controller. Based on the selected control method and parameter settings, the controller sent an output command to the solid-state relay to regulate the electrical power supplied to the heating element. The computer was connected to the controller through the RS-485 communication module for temperature monitoring, data logging, and supervisory control. The same hardware configuration was used for conventional PID, adaptive PID, and ON/OFF hysteresis control. The primary differences among the experiments were the control mode and the parameter-setting mechanism applied in the Autonics controller.

The fixed process settings included a methanol-to-oil molar ratio of 9:1, a nominal stirring speed of 600 rpm, a heating-element rated power of 350 W, a reaction time of 40 min, and a NaOH catalyst concentration of 1% (w/w) relative to the oil mass. The experimental factors were the reaction-temperature setpoint, vegetable-oil feedstock, and temperature-control method. The temperature setpoints were 50°C and 60°C, the feedstocks were palm oil and castor oil, and the tested control methods were conventional PID, adaptive PID, and ON/OFF hysteresis control. The evaluated outcomes were the observed temperature response and recovered biodiesel yield. Temperature response was described using rise time, overshoot, settling time, and steady-state error. Energy consumption was not included as an experimental outcome because electrical-energy input, controller-output percentage, and synchronized heater-duty-cycle data were not measured for each run. The experimental factors consisted of temperature-control method, feedstock type, and reaction temperature, as shown in Table 3. The study evaluated all 3 × 2 × 2 combinations of three control methods, two feedstocks, and two temperature setpoints, resulting in 12 experimental conditions. Each condition was evaluated in a single experimental run. Therefore, the results were interpreted descriptively, and experimental error, confidence intervals, and interaction effects were not estimated.

Table 3 Experimental treatment combinations

Experiment	Control Method	Temperature (°C)	Feedstock
Baseline	PID	50	Sunflower oil
1	PID	50	Castor oil
2	PID	50	Palm oil
3	PID	60	Castor oil
4	PID	60	Palm oil

5	Adaptive PID	50	Castor oil
6	Adaptive PID	50	Palm oil
7	Adaptive PID	60	Castor oil
8	Adaptive PID	60	Palm oil
9	Hysteresis	50	Castor oil
10	Hysteresis	50	Palm oil
11	Hysteresis	60	Castor oil
12	Hysteresis	60	Palm oil

Table 3 presents the experimental variables evaluated in this study. The main experiment included all 3 × 2 × 2 combinations of three temperature-control methods, two reaction-temperature setpoints, and two feedstocks, resulting in 12 experimental conditions. The control methods were conventional PID, adaptive PID, and hysteresis control. The temperature setpoints were 50 °C and 60 °C, while the feedstocks were palm oil and castor oil. Each experimental condition was evaluated in a single run. Sunflower oil at a setpoint of 50 °C was used only during the preliminary autotuning stage to obtain an initial PID parameter set before the main experiment. This condition was selected as a standardized preliminary test because the initial controller commissioning and autotuning procedure were performed using sunflower oil at the lower operating setpoint of the study. The resulting parameters were subsequently adopted as a common baseline for all main experiments to ensure a consistent initial controller configuration. This selection does not imply that sunflower oil at 50 °C was the optimal or most representative condition for all feedstocks and setpoints.

The autotuning procedure produced PID parameters of P = 4.9, I = 359 s, and D = 75 s, resulting in a rise time of 3 min, an overshoot of 1 °C, a settling time of 4 min, and a steady-state error of 0.055 °C. Because overshoot was still observed, two manual tuning trials were subsequently conducted. In the first trial, the proportional gain was increased to P = 5.5, while the integral and derivative gains remained unchanged. This adjustment reduced the rise time to 2.5 min, eliminated the overshoot, and shortened the settling time to 3 min, although the steady-state error increased to 0.067 °C. In the second trial, the proportional gain was reduced to P = 5.2, whereas I = 359 s and D = 75 s were retained. This configuration maintained a rise time of 2.5 min, eliminated overshoot, achieved a settling time of 3 min, and reduced the steady-state error to 0.040 °C. Therefore, P = 5.2, I = 359 s, and D = 75 s were selected as the final baseline PID parameters because they provided the best overall control performance among the evaluated settings. These parameters were subsequently used as identical initial settings for both the conventional and adaptive PID controllers, ensuring that differences in temperature responses reflected the effects of the control strategy and feedstock characteristics rather than variations in the initial controller configuration. Nevertheless, because the baseline parameters were obtained using sunflower oil at only one operating condition, their suitability for palm oil and castor oil at different setpoints was not independently evaluated and is acknowledged as a limitation of this study.

The experimental procedure began with the autotuning process on the Autonics temperature controller to obtain the reference PID parameters. The transesterification experiments were then performed using conventional PID, adaptive PID, or hysteresis control according to the assigned experimental condition. After the reactants were introduced into the reactor, heating and mixing were initiated simultaneously, and the reaction time of 40 min was measured from the start of both processes. Temperature data were continuously recorded throughout the experiment. Rise time and overshoot were evaluated during the heating stage, whereas settling time and steady-state error were assessed after the reactor temperature approached the setpoint and throughout the remaining reaction period. Upon completion of the transesterification process, the biodiesel product was washed with distilled water and transferred to a separating funnel until complete phase separation was achieved. The upper biodiesel layer was subsequently collected for density measurement and biodiesel yield determination.

Conventional PID Temperature Control Process

The traditional PID control method consisted of the measurement of the reactor temperature by a Type-K thermocouple connected directly to the Autonics temperature controller. The process variable (PV) was the measured temperature, which was continuously compared to the predetermined setpoint value (SV). The control error was defined as the difference between the PV and SV and was used as the input for the proportional, integral and derivative control actions. Based on this mistake, the control output was continuously adjusted by the controller to minimize the temperature deviation and to maintain stable reactor operation during biodiesel production process. The control output from the PID algorithm was sent to the solid-state relay (SSR) which controlled the AC electrical power supplied to the heating element. While reducing the overshoot and steady state error, the controller was able to keep the temperature of the reactor close to the required setpoint by modulating the heater power continuously. The temperature control process in this study is based on the conventional closed loop process of sensing, error calculation, PID calculation and heater actuation. Figure 5 shows the supervisory process of conventional PID temperature-control process.

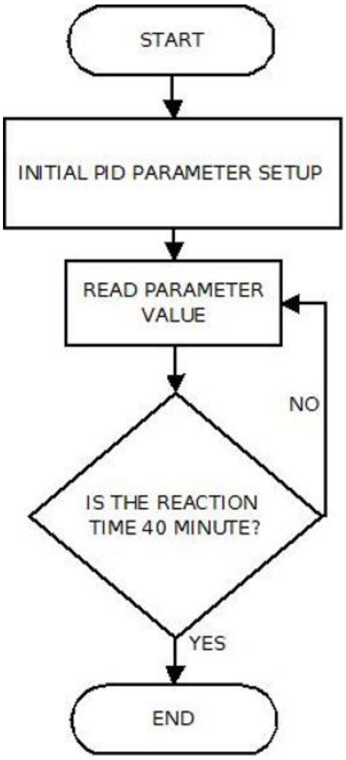

Figure 5 Conventional PID Temperature-Control Workflow

In conventional PID control, the process began with the initialization of the baseline controller parameters, namely P = 5.2, I = 359 s, and D = 75 s. These parameters were obtained through a baseline PID tuning procedure that began with the built-in autotuning function of the Autonics TK4S and was followed by two manual tuning trials. During the transesterification experiment, the process variable (PV) was continuously read from the Type-K thermocouple and processed by the Autonics controller using the fixed baseline PID parameters. The control loop was repeated throughout the heating and reaction process until the reaction time reached 40 min. The baseline parameters were retained without online adjustment or re-tuning for all conventional PID experiments using palm oil and castor oil at setpoints of 50 °C and 60 °C.

$$u(t) = K_p e(t) + K_i \int e(t)dt + K_d \frac{de(t)}{dt} \quad (1)$$

where $u(t)$ is the control output signal, K_p is the proportional parameter that remains constant, K_i is the integral parameter that remains constant, K_d is the derivative parameter that remains constant, and $e(t)$ is the error between the set value (SV) and the process value (PV).

Adaptive PID Temperature Control Process

The adaptive PID method used the Autonics TK4S as the primary controller, while an external supervisory layer implemented on the computer adjusted the PID settings online during the heating process. The initial controller settings were taken from the baseline tuning result, namely P=5.2, I=359 s, and D=75 s. The supervisory algorithm evaluated the process temperature, temperature rate of change, proximity to the setpoint, overshoot, and steady-state error. During the initial heating stage, the temperature response was evaluated every 60 s. When the process temperature approached the setpoint, the evaluation interval was changed to 120 s. The supervisory workflow of the adaptive PID temperature-control process is presented in Figure 6, while the corresponding pseudocode is summarized in Table 4.

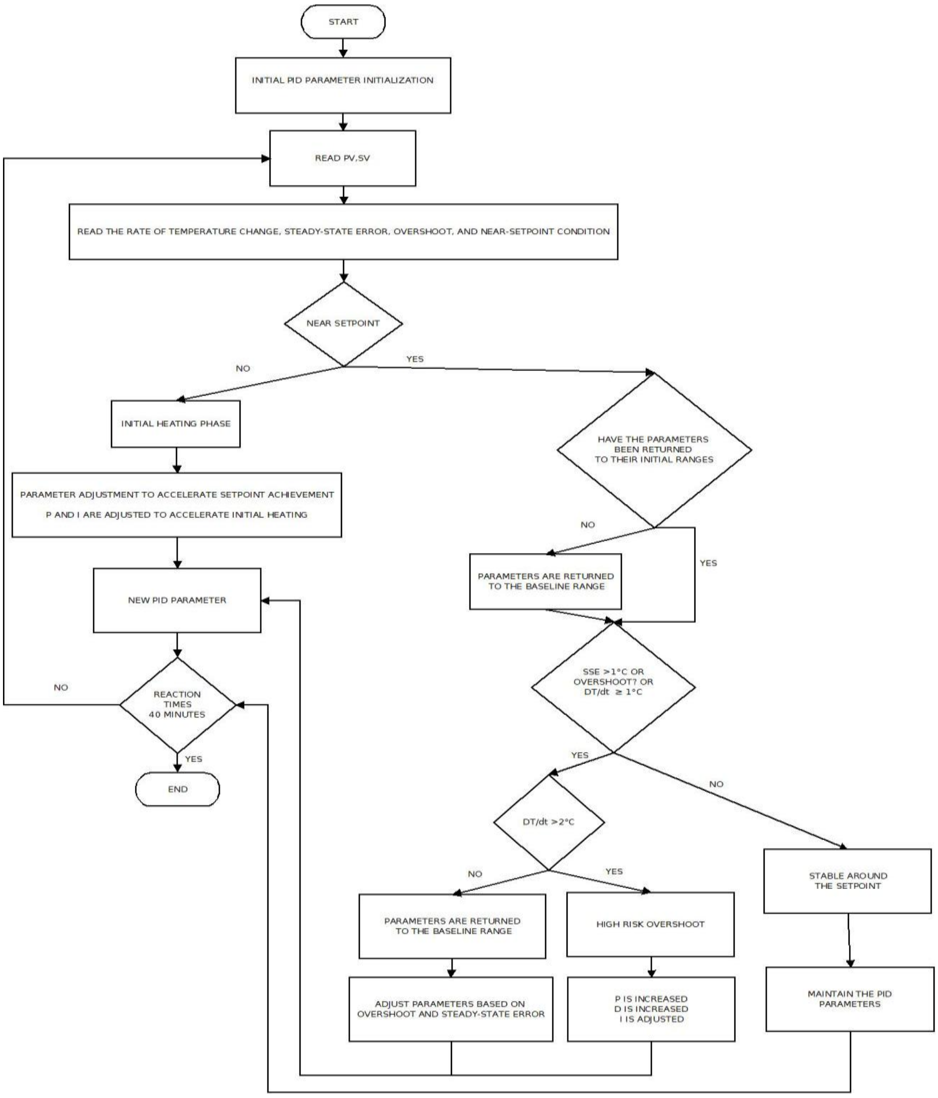

Figure 6 Adaptive PID Temperature-Control Workflow

Figure 6 illustrates the workflow of the proposed Supervisory Adaptive PID controller, showing how the temperature error is monitored, system performance is evaluated, and the PID parameters are adaptively updated to achieve stable and accurate temperature regulation. To facilitate implementation, the corresponding algorithm is presented as pseudocode in Table 4.

Table 4 Supervisory Adaptive PID Pseudocode

Step	Procedure
1	Initialize baseline parameters: P = 5.2, I = 359 s, and D = 75 s.
2	Define the adjustment limits: P ±30%, I ±25%, and D ±20% relative to the baseline values.
3	Start heating, mixing, and temperature-data acquisition.
4	Read PV, SV, and the current P, I, and D settings.
5	Calculate the temperature rate of change, overshoot condition, and steady-state error.
6	Determine the operating phase based on the temperature response.
7	Use a 60 s evaluation interval during the initial heating phase and a 120 s interval near the setpoint.
8	Send the structured process information to the Llama 3.1 8B Instruct supervisory model.
9	Receive the proposed adjustment decision for P, I, and D
10	Check the output format and verify that the proposed values remain within the permitted
11	If the output is valid, transmit the updated parameters to the Autonics TK4S through RS-485 Modbus RTU communication.
12	If the output is invalid or exceeds the limits, retain the previous valid parameters.
13	If the stability criteria are satisfied, maintain the current parameters.
14	Repeat Steps 4–13 until the reaction time reaches 40 min.
15	Stop data acquisition and end the experiment.

As shown in Figure 6, the adaptive PID supervisory process evaluated the process temperature, temperature rate of change, proximity to the setpoint, overshoot, steady-state error, and current PID settings to determine whether parameter adjustment was required. During the initial heating phase, P and D were adjusted within the predefined limits to accelerate the temperature response. When the process temperature entered the near-setpoint region, defined as PV ≥ SV − 2 °C, the PID settings were gradually returned toward their baseline values. If overshoot or a tendency toward overshoot was detected, P was increased to weaken the proportional action, I was temporarily reduced to limit integral accumulation, and D was increased to provide additional damping. When the predefined stability criteria were satisfied, the supervisory system entered a hold condition and maintained the current parameter values.

The supervisory decision-making process was performed using a locally executed Llama 3.1 8B Instruct model integrated with a Python 3.11 application. At each evaluation interval, the model received structured process information consisting of the process temperature, setpoint, temperature rate of change, overshoot condition, steady-state error, current PID settings, and operating phase. Based on predefined supervisory instructions, the model generated adjustment decisions for P, I, and D. The model did not directly control the heater or solid-state relay. Python handled data acquisition, preparation of the model input, parsing of the model output, validation of the proposed parameter values, and transmission of the accepted settings to the Autonics TK4S through RS-485 Modbus RTU communication. All parameter adjustments were constrained relative to the baseline settings, with limits of ±30% for P, ±25% for I, and ±20% for D. Near the setpoint, parameter changes were limited to approximately ±5% of the baseline values. Outputs that exceeded the permitted limits, contained invalid values, or did not follow the predefined format were rejected, and the previous valid settings were retained. After validation, the accepted parameters were transmitted to the Autonics TK4S, which continued to execute its built-in PID calculation using the most recently accepted settings. The RS-485 communication delay was not measured independently; therefore, no quantitative latency value is reported. The internal anti-windup, output-saturation, and derivative-filtering functions of the commercial controller were not modified or separately characterized. The adaptive PID control action is expressed by Equation (2) (Landau et al., 2011).

$$u(t) = K_p(t)e(t) + K_i(t)\int e(t)dt + K_d(t)\frac{de(t)}{dt} \tag{2}$$

where $u(t)$ is the control output signal, $K_p(t)$ is the proportional parameter that varies over time, $K_i(t)$ is the integral parameter that varies over time, $K_d(t)$ is the derivative parameter that varies over time, and $e(t)$ is the error between the set value (SV) and the process value (PV).

Hysteresis Temperature Control Process

The reactor temperature was controlled by an Autonics controller based on the ON/OFF hysteresis control strategy. The control action was established by the predefined temperature setpoint and the selected hysteresis band. The reactor temperature was continuously measured by a type-K thermocouple directly connected to the Autonics controller. Compared with continuous control strategies, the hysteresis control keeps the current state of the heating element until the measured temperature reaches the upper or lower threshold of the hysteresis band. This leads to a lower switching frequency of the heating element, which improves the durability of the actuator and ensures good temperature stability throughout the whole biodiesel production process. The hysteresis band was first tuned in an effort to guarantee stable operation during the heating phase and then tuned according to the measured temperature response. When the reactor temperature approached the target setpoint a narrower hysteresis band was used for better control accuracy and a wider hysteresis band was used for larger temperature deviations to avoid excessive switching and unnecessary operation of the actuator. This adaptive hysteresis strategy offers an efficient trade-off between the accuracy of temperature regulation, energy efficiency, and operational lifetime of the switching components. The supervisory workflow of the proposed hysteresis control strategy is shown in Fig. 7, and the corresponding implementation procedure is summarized as pseudocode in Table 5.

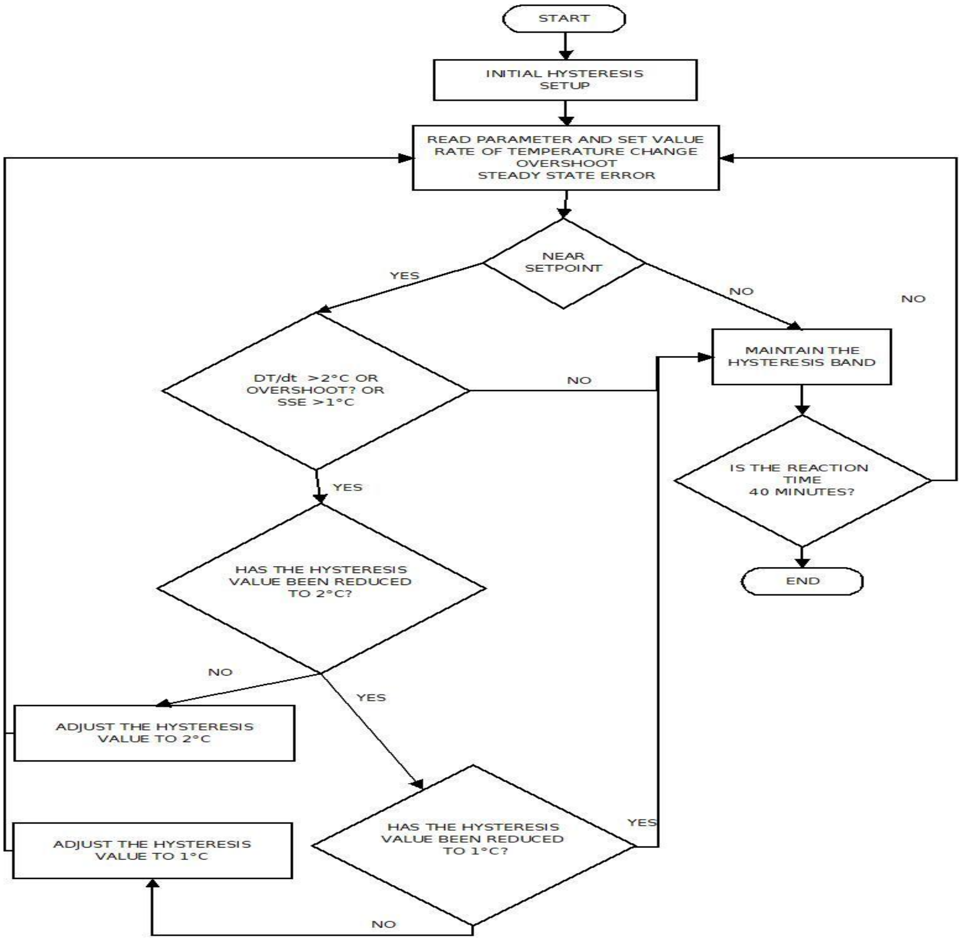

Figure 7 Hysteresis Temperature-Control Workflow

Figure 7 illustrates the workflow of the proposed hysteresis temperature-control strategy, showing how the hysteresis band is adjusted according to the system response to improve temperature stability while minimizing unnecessary switching. The implementation procedure of this control strategy is presented as pseudocode in Table 5.

Table 5 Hysteresis Temperature-Control Pseudocode

Step	Procedure
1	Initialize the hysteresis band (HYS = 3 °C).
2	Start the heating process, agitator, and temperature-data acquisition.
3	Read the process value (PV), setpoint value (SV), current HYS, and temperature-response indicators.

4	Define the switching thresholds: Upper = SV and Lower = SV – HYS.
5	If PV ≤ Lower, activate the SSR and turn the heater ON.
6	Else if PV ≥ Upper, deactivate the SSR and turn the heater OFF.
7	Otherwise, maintain the previous heater state.
8	Check whether the process has entered the near-setpoint region (PV ≥ SV – 2 °C).
9	If the near-setpoint region has not been reached, retain the current HYS value.
10	Otherwise, evaluate the temperature rate of change (dT/dt), overshoot, and steady-state error (SSE).
11	If dT/dt > 2 °C/min, overshoot is detected, or |SSE| > 1 °C, update the hysteresis band according to the supervisory rules.
12	If HYS = 3 °C, reduce HYS to 2 °C.
13	Else if HYS = 2 °C and overshoot persists during the next heating cycle, reduce HYS to 1 °C; otherwise, retain the current HYS value.
14	If HYS = 1 °C, maintain the minimum hysteresis band.
15	Transmit the updated HYS value to the Autonics TK4S via RS-485 Modbus RTU communication.
16	Repeat Steps 3–15 until the reaction time reaches 40 min.
17	Stop temperature-data acquisition and terminate the experiment.

As shown in Figure 7, the hysteresis-control process began with the initialization of the hysteresis band at 3 °C. During the reaction, the process value (PV), set value (SV), temperature rate of change, overshoot condition, and steady-state error were monitored. While the reactor temperature remained outside the near-setpoint region, the initial hysteresis value was maintained. The near-setpoint region was defined as PV ≥ SV − 2 °C. After this condition was reached, the supervisory system evaluated the temperature response to determine whether the hysteresis band required adjustment. The Autonics TK4S performed the ON/OFF heater-switching action according to the upper and lower limits defined by the current hysteresis value. The upper and lower switching limits are expressed by Equation (3) (Seborg et al., 2011).

$$T_{upper} = T_{set}$$

$$T_{lower} = T_{set} - HYS \tag{3}$$

where T_{upper} is the upper switching limit at which the heater is turned off, T_{lower} is the lower switching limit at which the heater is turned on, T_{set} is the temperature setpoint, and HYS is the hysteresis-band width. All variables are expressed in degrees Celsius (°C). Accordingly, the heater is activated when $PV \leq T_{\text{lower}}$ and deactivated when $PV \geq T_{\text{upper}}$. For example, at $T_{set} = 60^{\circ}\text{C}$ and $HYS = 3^{\circ}\text{C}$, the heater is activated when PV decreases to 57°C or below and is deactivated when PV reaches 60°C. This mechanism prevents repeated switching at a single temperature threshold. When the near-setpoint condition was reached, the supervisory system evaluated the temperature rate of change, overshoot behavior, and steady-state error. If the temperature rate of change exceeded 2 °C/min, an overshoot tendency was detected, or the absolute steady-state error exceeded 1 °C, HYS was reduced from 3 °C to 2 °C. Otherwise, HYS remained at 3 °C. After HYS had been reduced to 2 °C, the system monitored the temperature response for one complete heating cycle. A heating cycle began when the heater was reactivated after PV reached the lower switching limit and ended when the heater was deactivated after PV reached the upper switching limit. If overshoot occurred again during the following heating cycle, HYS was further reduced from 2 °C to 1 °C. If no further overshoot was observed, HYS remained at 2 °C. Once HYS reached 1 °C, it was maintained for the remainder of the process. Thus, the hysteresis band was adjusted within the range of 1–3 °C according to proximity to the setpoint, temperature rate of change, overshoot behavior, and steady-state error. The Autonics TK4S continued to perform real-time ON/OFF switching, while the computer evaluated the recorded temperature response and transmitted the updated HYS value through RS-485 communication using the Modbus RTU protocol. This supervisory evaluation and switching process was repeated until the reaction time reached 40 min.

Data Analysis

The parameters analyzed in this study included temperature response, biodiesel density, and biodiesel yield. The temperature response was evaluated using rise time, overshoot, settling time, and steady-state error. Rise time was defined as the time required for the measured temperature to increase from 10% to 90% of the total temperature change between the initial temperature and the setpoint (Ogata., 2010). Settling time was defined as the time at which the measured temperature first entered and subsequently remained within a fixed ±3°C band around the setpoint. A ±3°C band was used consistently for the 50°C and 60°C setpoints because the recorded temperature values were available in whole-degree increments. Steady-state error was calculated using Equation (4) as the difference between the setpoint and the average measured temperature after the system had reached the settling condition (Ogata., 2010).

$$e_{ss} = \frac{1}{N}\sum_{i=1}^{N}(SV - PV_i) \tag{4}$$

where e_{ss} is the steady-state error, N is the number of temperature data points collected after the settling condition was reached, SV is the setpoint value, and PV_i is the measured process value at the i-th observation.

Result and Discussion

PID, Adaptive PID, and Hysteresis Temperature Control Performance

The temperature-response profiles for all 12 experimental conditions are provided in Figures S1–S12 of the Supplementary Material, while the corresponding response parameters are summarized in Figures 8–13. Rise time was analyzed to evaluate the speed of the temperature control system in reaching the target temperature. A lower rise time value indicates that the system is able to approach the setpoint more quickly during the heating process. The rise time test results are shown in Figure 8.

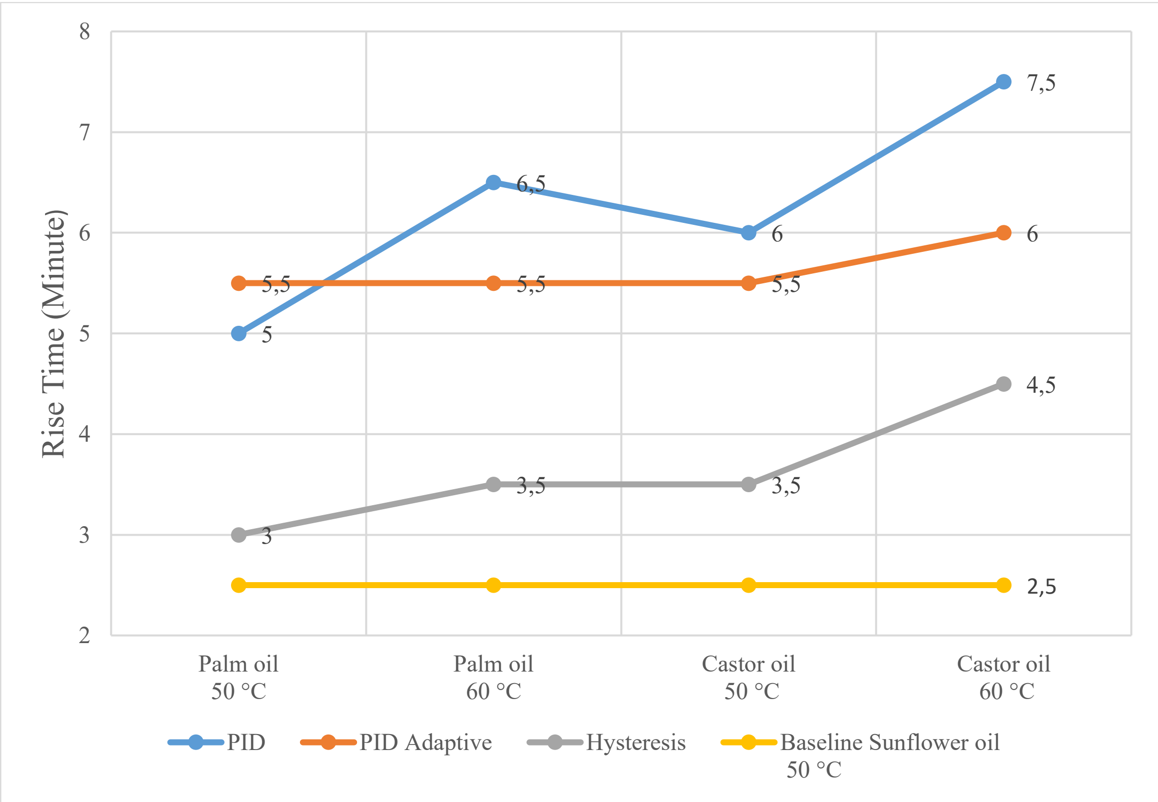

Figure 8 Rise Time under Different Experimental Variables

Figure 8 presents the observed rise-time values for each experimental condition. The reference test using sunflower oil at 50°C produced a rise time of 2.5 min. For palm oil at 50°C, the observed rise times were 5 min for conventional PID, 5.5 min for adaptive PID, and 3 min for hysteresis control. At 60°C, the corresponding values were 6.5, 5.5, and 3.5 min, respectively. For castor oil at 50°C, the observed rise times were 6 min for conventional PID, 5.5 min for adaptive PID, and 3.5 min for hysteresis control. At 60°C, the corresponding values were 7.5, 6, and 4.5 min, respectively. Among the tested single-run conditions, hysteresis control showed the lowest observed rise time, followed generally by adaptive PID and conventional PID. Longer rise times were observed at the 60°C setpoint than at 50°C for most tested conditions, indicating that more time was required for the measured temperature to reach the higher target. Differences were also observed between palm oil and castor oil. However, because each condition was evaluated in a single experimental run, the thermal properties of the feedstocks were not independently characterized, and viscosity was not measured directly, the observed differences cannot be attributed conclusively to specific feedstock properties such as viscosity, heat-storage capacity, or heat-transfer behavior. Settling time was used to describe the time required for the measured temperature to enter and remain within the predefined settling band around the setpoint. A lower settling-time value indicates that the measured response reached this condition more quickly. The observed settling-time values are presented in Figure 9.

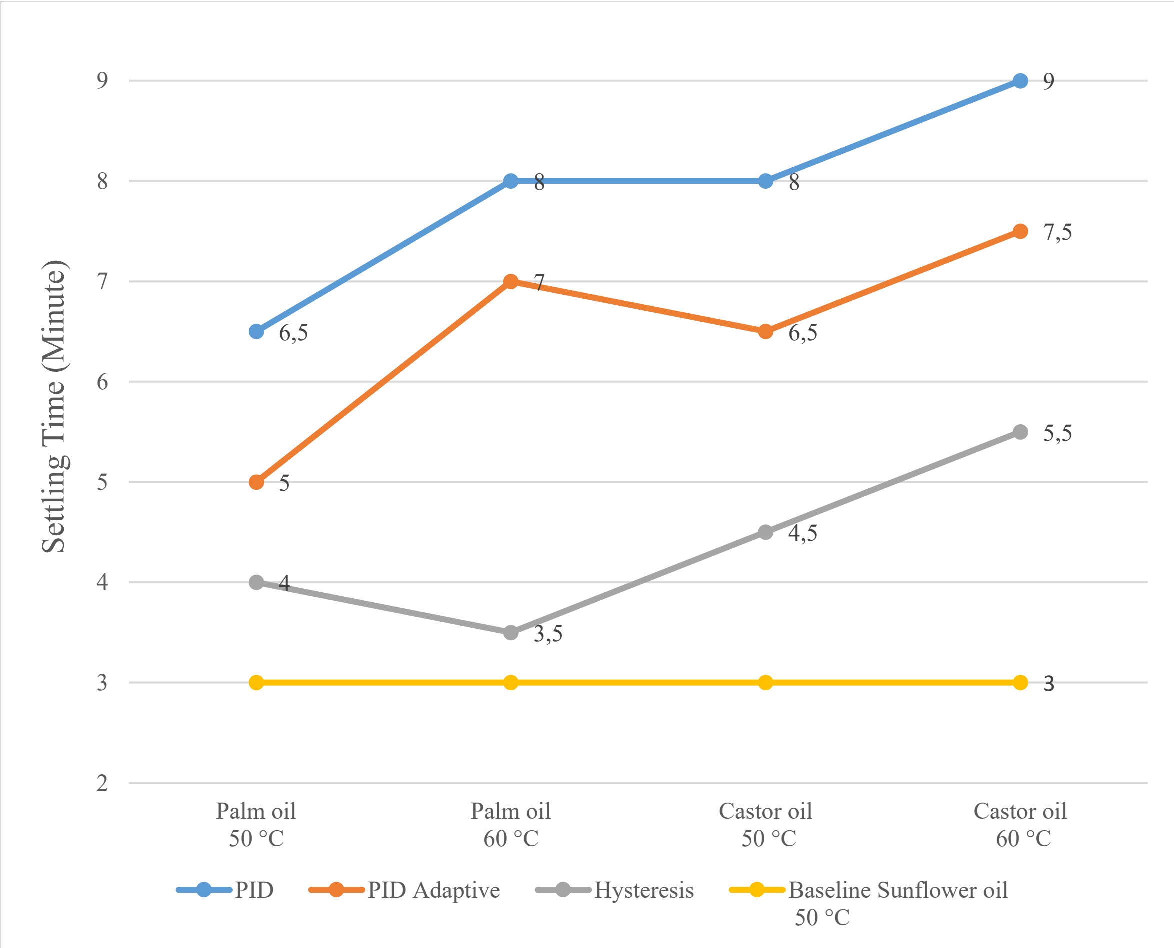

Figure 9 Settling Time under Different Experimental Variables

Figure 9 presents the observed settling-time values for each experimental condition. The reference test using sunflower oil at 50°C produced a settling time of 3 min. For palm oil at 50°C, the observed settling times were 6.5 min for conventional PID, 5 min for adaptive PID, and 4 min for hysteresis control. At 60°C, the corresponding values were 8, 7, and 3.5 min, respectively. For castor oil at 50°C, the observed settling times were 8 min for conventional PID, 6.5 min for adaptive PID, and 4.5 min for hysteresis control. At 60°C, the corresponding values were 9, 7.5, and 5.5 min, respectively. Among the tested single-run conditions, hysteresis control showed the lowest observed settling time under all tested conditions, followed by adaptive PID and conventional PID. For conventional PID and adaptive PID, longer settling times were observed at the 60°C setpoint than at 50°C. For hysteresis control, the settling time increased from 4.5 to 5.5 min for castor oil but decreased slightly from 4 to 3.5 min for palm oil. However, because each condition was evaluated in a single experimental run, the thermal properties of the feedstocks were not independently characterized, and viscosity was not measured directly, the observed differences between palm oil and castor oil cannot be attributed conclusively to specific feedstock properties. Overshoot was used to describe the extent to which the measured temperature exceeded the setpoint during the control process. A lower overshoot value indicates that the temperature response remained closer to the target without excessive temperature excursion. The observed overshoot values are presented in Figure 10.

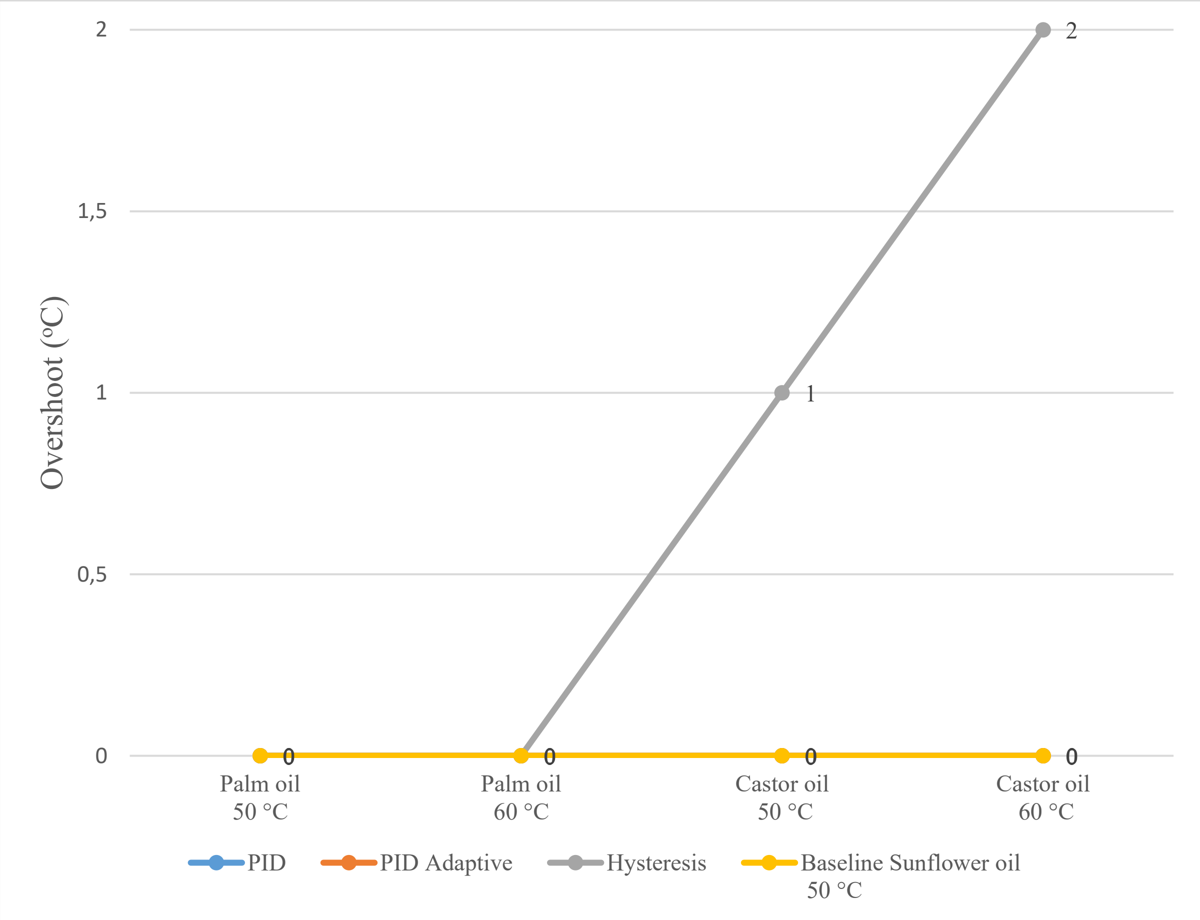

Figure 10 Overshoot under Different Experimental Variables

Figure 10 presents the observed overshoot values for each experimental condition. The reference test using sunflower oil at 50°C produced an overshoot of 0°C. Conventional PID and adaptive PID also showed no observed overshoot in the palm-oil and castor-oil tests at either 50°C or 60°C. Under the tested single-run conditions, the measured temperature therefore did not exceed the setpoint when these two control methods were applied. For hysteresis control, overshoot was observed in the castor-oil tests. The observed overshoot was 1°C at the 50°C setpoint and 2°C at the 60°C setpoint. These values remained below the 5% tolerance limits of 2.5°C and 3°C for the 50°C and 60°C setpoints, respectively. The ON/OFF switching mechanism and residual heat after the heating element was switched off may have contributed to the observed temperature excursion. However, because heater thermal inertia and heat-transfer behavior were not independently measured, this mechanism cannot be confirmed conclusively from the present data. Among the tested single-run conditions, conventional PID and adaptive PID showed lower observed overshoot than hysteresis control because no overshoot was recorded for either method. However, each condition was evaluated in only one experimental run; therefore, these results should be interpreted as descriptive observations rather than statistically validated performance differences. Steady-state error was used to describe the difference between the setpoint and the measured temperature after the response had entered the stable region. A lower steady-state error indicates that the measured temperature remained closer to the setpoint. The observed steady-state error values are presented in Figure 11.

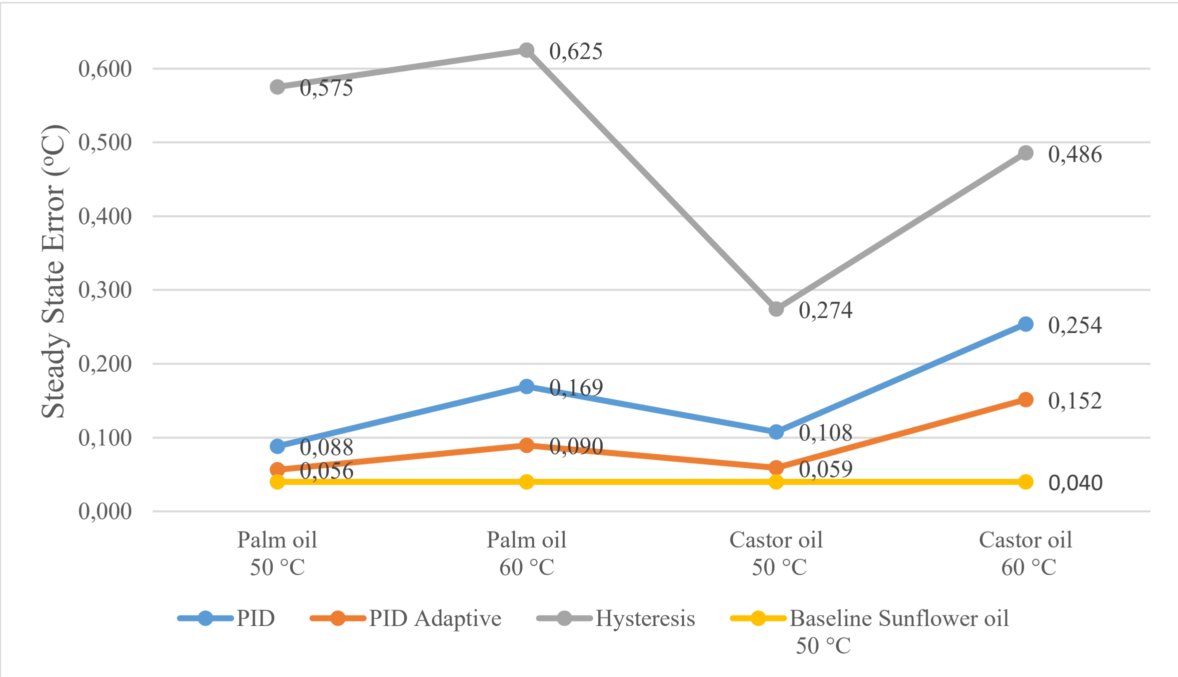

Figure 11 Steady State Error under Different Experimental Variables

Figure 11 presents the steady-state error values calculated using Equation (4) from the controller-indicated temperature data during the steady-state interval. The reference test using sunflower oil at 50°C produced a calculated steady-state error of 0.040°C. For palm oil at 50°C, the calculated steady-state errors were 0.088°C for conventional PID, 0.056°C for adaptive PID, and 0.575°C for hysteresis control. At 60°C, the corresponding values were 0.169, 0.090, and 0.625°C, respectively. These values represent averages calculated from multiple temperature readings rather than individual sensor readings. However, values smaller than the stated thermocouple accuracy should be interpreted cautiously because averaging does not eliminate the measurement uncertainty of the thermocouple–controller–data-acquisition chain. For castor oil, the steady-state error at 50°C was 0.108°C for conventional PID, 0.059°C for adaptive PID, and 0.274°C for hysteresis control. At 60°C, the steady-state error values were 0.254°C, 0.152°C, and 0.486°C, respectively. Overall, adaptive PID produced the lowest steady-state error, followed by conventional PID and hysteresis control. Under the tested single-run conditions, adaptive PID showed the lowest calculated controller-indicated steady-state error values. However, all steady-state error values remained below the tolerance limit of 2% of the setpoint; therefore, the system can generally be considered stable. The controller comparison covered the complete 40 min reaction period, beginning when heating and mixing were started after the reactants had been introduced. Rise time and overshoot were used to characterize the initial heat-up phase, whereas settling time and steady-state error were used to evaluate the response after the temperature approached the setpoint and during the remaining reaction-holding period. Overall, palm oil and castor oil showed longer observed rise times and settling times than the sunflower-oil reference test at 50°C. Among the tested single-run conditions, adaptive PID showed no observed overshoot and the lowest calculated controller-indicated steady-state error values, whereas hysteresis control showed the shortest rise and settling times but larger steady-state errors and overshoot in the castor-oil tests. Conventional PID also maintained the recorded temperature without overshoot, although its rise and settling times were generally longer than those observed with adaptive PID. During the reaction-holding period, temperature stability was assessed from the recorded temperature data after the response had entered and remained within the predefined settling band. Because each condition was evaluated in a single run and the measurement uncertainty of the complete temperature-measurement chain was not independently established, these results are presented as descriptive observations rather than definitive statistical performance rankings.

Biodiesel Density and Yield

The density of the crude biodiesel was measured at 30°C using a 25 ml pycnometer. The empty, clean, and dry pycnometer was weighed to obtain m_p. The pycnometer was then filled with distilled water and weighed to obtain m_w. Subsequently, the pycnometer was filled with the crude biodiesel sample and weighed to obtain m_s. The sample density was calculated using Equation (5).

$$\rho_s = \frac{ms - m_p}{mw - m_p} \times \rho_w \quad (5)$$

where ρ_s is the density of the crude biodiesel sample (g/cm³), m_p is the mass of the empty pycnometer (g), m_w is the mass of the pycnometer filled with distilled water (g), m_s is the mass of the pycnometer filled with the crude biodiesel sample (g), and ρ_w is the density of distilled water at the measurement temperature (g/cm³). The biodiesel density test results are shown in Figure 12.

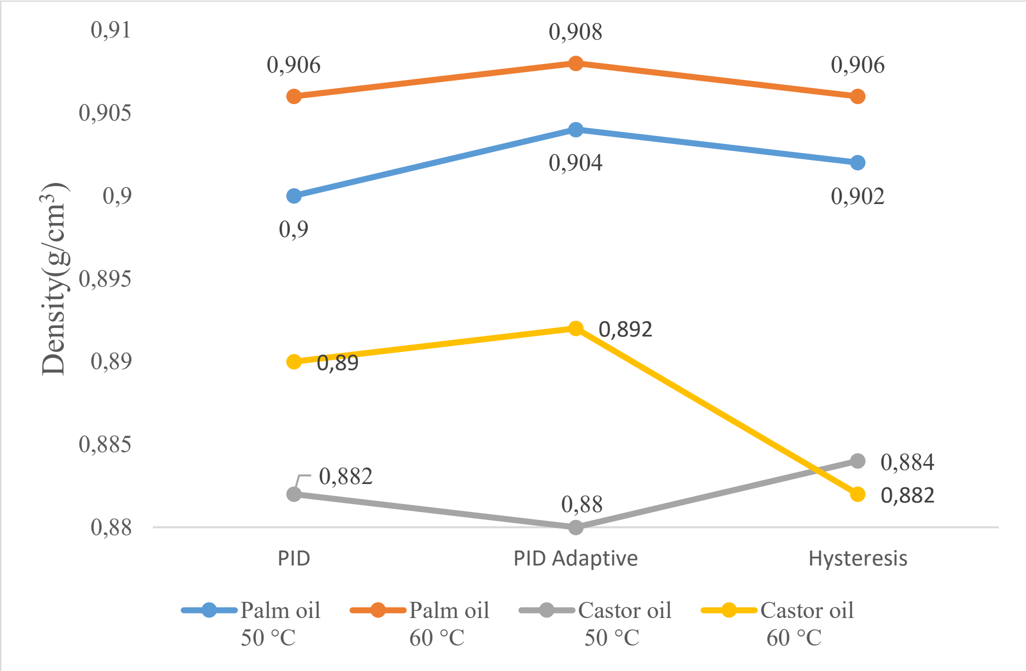

Figure 12 Biodiesel Density

Figure 12 presents the measured density values of the crude biodiesel obtained under each temperature-control condition. The observed values ranged from 0.880 to 0.908 g/cm³. The palm-oil-derived products showed density values between 0.900 and 0.908 g/cm³, whereas the castor-oil-derived products showed values between 0.880 and 0.892 g/cm³. The lowest observed density, 0.880 g/cm³, was obtained from castor oil using adaptive PID control at 50°C, while the highest observed density, 0.908 g/cm³, was obtained from palm oil using adaptive PID control at 60°C. For palm oil, the observed density increased from 0.900 to 0.906 g/cm³ under conventional PID control, from 0.904 to 0.908 g/cm³ under adaptive PID control, and from 0.902 to 0.906 g/cm³ under hysteresis control when the reaction temperature was increased from 50°C to 60°C. Differences were also observed between palm-oil-derived and castor-oil-derived products. However, because each condition was evaluated in a single experimental run and the feedstock properties, including water content, acid value, free-fatty-acid content, initial density, viscosity, and fatty-acid composition, were not independently characterized, the observed density differences cannot be attributed conclusively to feedstock type, reaction temperature, or temperature-control performance.

The palm oil and castor oil used in this study were commercially available feedstocks selected based on the applicable Indonesian quality specifications stated by the suppliers. However, conformity with specific SNI parameters was not independently verified. Therefore, the density results are reported as descriptive measurements of crude biodiesel and are not used to claim compliance with a specific biodiesel standard. After the 40 min transesterification reaction was completed, the reaction mixture was transferred directly to a separating funnel. Distilled water at 60°C was then added using a water-to-reaction-mixture volume ratio of 1:1 (v/v). The contents of the separating funnel were gently agitated for approximately 2 min to promote contact between the aqueous and organic phases while minimizing emulsion formation. The mixture was subsequently allowed to stand for 24 h until distinct layers were formed. The lower aqueous and glycerol-rich phase was removed by gravity, while the upper crude biodiesel phase was collected. The recovered biodiesel was then heated at 100°C for 30 min while being stirred manually to maintain uniform mixing and reduce residual water and volatile components, following the general purification procedure reported by (Arenas et al.,2021). Yield was used to evaluate the amount of biodiesel produced under each experimental condition. Biodiesel yield was calculated using Equation (6).

$$Yield(\%) = \frac{m_b}{m_o} . 100\% \tag{6}$$

where $m_b$is the mass of the recovered and dried crude biodiesel (g), and $m_o$is the initial mass of vegetable oil used in the reaction (g). Yield was used to evaluate the amount of biodiesel recovered under each experimental condition. The biodiesel yield results are shown in Figure 12. The initial oil mass and final dried crude biodiesel mass for each experimental condition are provided in Table S1 of the Supplementary Material.

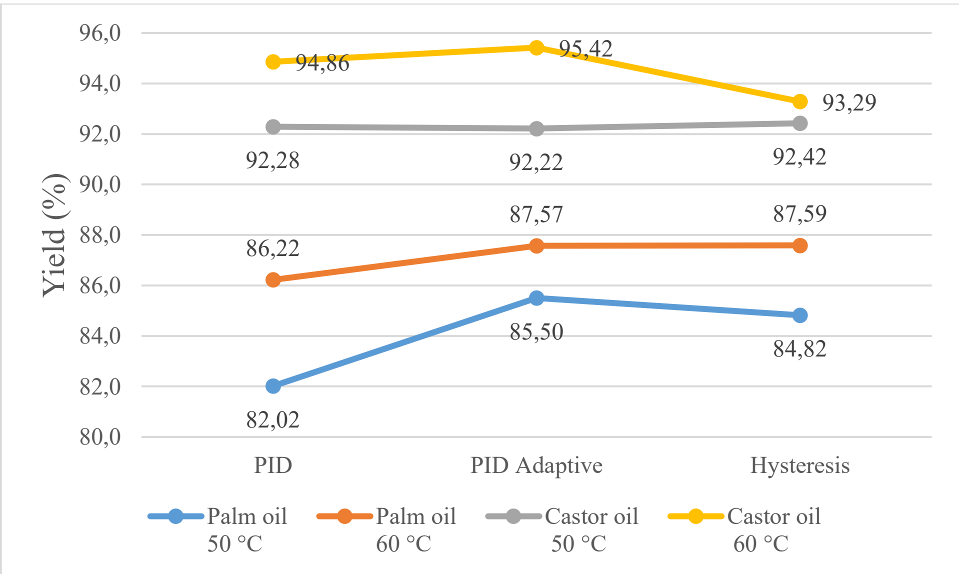

Figure 13 Biodiesel Yield

Figure 13 shows the biodiesel yield obtained under variations in feedstock, temperature setpoint, and control method. The highest biodiesel yield was obtained from castor oil using adaptive PID control at 60°C, with a value of 95.423%. The lowest yield was obtained from palm oil using conventional PID control at 50°C, with a value of 82.017%. In general, castor oil produced a higher yield than palm oil under the same control method and temperature setpoint. This difference may be influenced by feedstock characteristics, such as fatty acid composition and physical properties, which affect the mixing process and the contact between oil, methanol, and catalyst during transesterification (Angassa, 2023). Increasing the setpoint from 50°C to 60°C was generally accompanied by higher observed biodiesel yield values, which is consistent with the role of temperature in promoting the transesterification reaction (Ojha et al., 2024). For castor oil at 60°C, hysteresis control produced an observed yield of 93.285%, which was lower than the value obtained using adaptive PID under the same condition. Overall, adaptive PID showed the highest observed yield under several tested conditions, while the effects of control method, feedstock type, and reaction temperature should be interpreted descriptively because each experimental condition was evaluated in a single run.

Study Limitations

This study has several limitations. Each experimental condition was evaluated in a single run; therefore, experimental variability, confidence intervals, and statistical significance could not be determined. The thermocouple–controller–data-acquisition chain was not calibrated against a traceable reference, so small differences in the calculated steady-state error should be interpreted cautiously. The feedstocks were not independently characterized for viscosity, water content, acid value, or fatty-acid composition, and a complete batch mass balance was not performed. In addition, the recovered product was evaluated only based on density and mass-based yield; therefore, it is described as crude biodiesel rather than a fully characterized fuel product. These limitations restrict the generalization of the results beyond the tested laboratory-scale conditions.

Conclusions

The conventional PID, adaptive PID, and ON/OFF hysteresis temperature-control systems were implemented in a laboratory-scale vegetable-oil biodiesel transesterification process. The same reactor hardware was used at setpoints of 50°C and 60°C, while the control methods differed in their parameter-setting and switching mechanisms. Under the tested conditions, conventional PID and adaptive PID produced no observed overshoot. Adaptive PID showed the lowest calculated controller-indicated steady-state error, while hysteresis control produced the shortest observed rise and settling times but showed larger steady-state errors and overshoot in several castor-oil experiments. Because each experimental condition was evaluated in a single run and the complete measurement chain was not traceably calibrated, these results should be interpreted as descriptive observations rather than statistically or metrologically confirmed differences. The observed recovered crude-biodiesel yield was generally higher at 60°C than at 50°C and was higher for castor oil than for palm oil under the tested conditions. Adaptive PID produced the highest average observed yield among the three control methods. The highest observed yield was obtained using castor oil at 60°C with adaptive PID control. These findings do not establish statistical effects or an optimal operating condition because no independent replication or inferential statistical analysis was performed.

Future studies should include replicated and randomized experiments, traceable calibration of the temperature-measurement chain, complete mass-balance evaluation, and additional product-characterization tests. The control methods may also be evaluated at larger reactor scales and compared with other strategies, such as model predictive control, using broader feedstock and operating-condition ranges.

Acknowledgements

The authors would like to express their sincere gratitude to Institut Sains dan Teknologi Nasional (ISTN), Mandala Bhumi Laboratory, and the lecturers for their support, guidance, and assistance throughout this research. In accordance with the direction of Mandala Bhumi Laboratory, the research data are openly available upon request from the laboratory for academic and research purposes.

References

Adriansyah, Y., Prayoga, S., & Wibisana, A. (2025). Implementation of PID adaptive control system for hexapod robot orientation. *Journal of Applied Electrical Engineering, 9*(1), 109–114. https://doi.org/10.30871/jaee.v9i1.9085

Angassa, K., Tesfay, E., Weldmichael, T. G., & Kebede, S. (2023). Response surface methodology process optimization of biodiesel production from castor seed oil. *Journal of Chemistry, 2023*, 6657732. https://doi.org/10.1155/2023/6657732

Andrews, J., & Jelley, N. (2007). *Energy science: Principles, technologies, and impacts*. Oxford University Press.

Arenas, E., Villafán-Cáceres, S. M., Rodríguez-Mejía, Y., García-Loyola, J. A., Masera, O., & Sandoval, G. (2021). Biodiesel dry purification using unconventional bioadsorbents. *Processes, 9*(2), 194.

Arif, T. M., & Rahim, M. A. (2025). Agentic AI for real-time adaptive PID control of a servo motor. *Actuators, 14*(9), 459. https://doi.org/10.3390/act14090459

ASTM International. (2024). *ASTM E230/E230M-23a: Standard specification for temperature-electromotive force (EMF) tables for standardized thermocouples*. ASTM International.

Badan Pengkajian dan Penerapan Teknologi. (2019). *Indonesia energy outlook*. BPPT.

Badan Standardisasi Nasional. (1990). *SNI 01-1904-1990: Minyak biji jarak*. Dewan Standardisasi Nasional.

Badan Standardisasi Nasional. (2019). *SNI 7709:2019: Minyak goreng sawit*. Badan Standardisasi Nasional.

Bentley, J. P. (2005). *Principles of measurement systems* (4th ed.). Pearson Education.

Çağatay, M. T., & Karacan, S. (2022). Experimental performances of nonlinear GPC and discrete-time PID in multivariate process: NARIMAX and ARX models in temperature control of reactive distillation column in synthesis of biodiesel from waste cooking oil. *Pamukkale University Journal of Engineering Sciences*, 28(7), 977–986.

Codex Alimentarius Commission. (1999). *Standard for named vegetable oils: CXS 210-1999*. Codex Alimentarius Commission.

Dewi, S. W., Pauzi, G. A., Junaidi, J., & Suciyati, S. W. (2022). Furnace control system using the TCN4S temperature controller. *Journal of Energy, Material, and Instrumentation Technology, 3*(3), 74–78. https://doi.org/10.23960/jemit.v3i3.104

Ekinci, S., Izci, D., Jabari, M., & Ma'arif, A. (2025). Enhanced temperature control of continuous stirred tank reactors with 2-DOF PID controller optimized by quadratic interpolation algorithm. *Journal of Robotics and Control, 6*(3). https://doi.org/10.18196/jrc.v6i3.26586

European Committee for Standardization. (2012). *EN 14214: Liquid petroleum products—Fatty acid methyl esters (FAME) for use in diesel engines and heating applications—Requirements and test methods*. European Committee for Standardization.

Fong, C. C., & Abu Bakar, B. (2023). Study of PID controller mode at biodiesel pilot plant at UTHM. *Progress in Engineering Application and Technology, 4*(1), 545–556.

Goel, V., & Kumar, S. (2026). Advanced predictive modelling of biodiesel yield using artificial neural networks for Karanja oil transesterification. *Measurement: Energy, 9*, 100088. https://doi.org/10.1016/j.meaene.2026.100088

Handoko, S., & Winardi, B. (2025). Comparison of conventional and adaptive hysteresis current control methods for power quality improvement using active filters. *Advance Sustainable Science Engineering and Technology, 7*(4), 0250403. https://doi.org/10.26877/asset.v7i4.1981

Haryono, Noviyanti, A. R., & Kurnia, I. (2025). Yield and characteristics of biodiesel from variations in the mass ratio of waste cooking oil mixtures with different waste sources through homogeneous catalyzed esterification and transesterification reactions. *Jurnal Teknologi Lingkungan, 26*(2), 164–172.

Landau, I. D., Lozano, R., M'Saad, M., & Karimi, A. (2011). *Adaptive control: Algorithms, analysis and applications* (2nd ed.). Springer.

Manimaran, M., Nagalakshmi, S., Vasanthi, S., & Muthukumar, N. (2023). Evolutionary algorithm-based model predictive control for a reactive distillation column in biodiesel production. *Automatika, 64*(3), 613–621. https://doi.org/10.1080/00051144.2 023.2 203566

Martínez-Sánchez, O., Gómez-Castro, F. I., & Ramírez-Corona, N. (2022). Plantwide control of a biodiesel production process with variable feedstock. *Chemical Engineering Research and Design, 185*, 377–390. https://doi.org/10.1016/j.cherd.2022.07.037

Maya-Rodriguez, M. C., Carvajal-Mariscal, I., López-Muñoz, R., Lopez-Pacheco, M. A., & Tolentino-Eslava, R. (2023). Temperature control of a chemical reactor based on neuro-fuzzy tuned with a metaheuristic technique to improve biodiesel production. *Energies, 16*(17), 6187. https://doi.org/10.3390/en16176187

Mhetras, N., & Gokhale, D. (2025). Sustainable biodiesel production: Importance of feedstock resources and production methods. *RSC Advances, 15*, 26739–26754.

Mohd Rozi bin Musa, A. R. S. (2023). Application of PD, PI, and PID control mode on vessel VE203 at biodiesel pilot plant. *Progress in Engineering Application and Technology, 4*(1), 526–537.

Montgomery, D. C. (2019). *Design and analysis of experiments* (10th ed.). John Wiley & Sons.

Naseef, H. H., & Tulimat, R. H. (2025). Transesterification and esterification for biodiesel production: A comprehensive review of catalysts and palm oil feedstocks. *Energy Conversion and Management: X, 26*, 100031. https://doi.org/10.1016/j.ecm x.2025.100031

Ogata, K. (2010). *Modern control engineering* (5th ed.). Prentice Hall.

Ojha, P., Poudel, D., Rokaya, A., Maharjan, S., Timsina, S., Poudel, A., Satyal, R., & Satyal, P. (2024). Chemical compositions and essential fatty acid analysis of selected vegetable oils and fats. *Compounds, 4*(1), 37–70. https://doi.org/10.3390/compounds4010003

Patti, M., Braccia, L., Feroldi, D., & Zumoffen, D. (2024). Hierarchical MPC-based control structure for continuous biodiesel production. *The Canadian Journal of Chemical Engineering, 102*, 3157–3172. https://doi.org/10.1002/cjce.25244

Rahman, M. S., Hossain, M. S., Rahman, A. N. M. M., & Moral, M. N. A. (2025). Optimization of catalysts in the production of biodiesel from castor oil: Towards sustainable energy. *Next Research, 2*(2), 100310. https://doi.org/10.1016/j.nexres.2025.100310

Seborg, D. E., Edgar, T. F., Mellichamp, D. A., & Doyle, F. J. (2011). *Process dynamics and control* (3rd ed.). John Wiley & Sons.

Sutapa, I. W., Bandjar, A., Tehubijuluw, H., Ely, I. S., Kamari, A., Baskar, C., Sudiana, I. N., & Kadidae, L. O. (2025). Transesterification reaction on biodiesel production from bintaro oil (*Cerbera manghas* L.) from Moluccas Island. *International Journal of Acta Material, 1*(2), 109–118. https://doi.org/10.62749/ijactmat.v1i2.15

Wen, H., Roberts, J., Zaidi, A., & McLeod, A. (2026). An experiment of using a large language model to control a water tank system. *Computers & Chemical Engineering*, 109656. https://doi.org/10.1016/j.compchemeng.2026.109656

Yang, Y., & Harper, J. (2024). Adaptive state feedback controller design for efficient biodiesel production under kinetic uncertainty. *Chemical Engineering Research and Design, 209*, 81–93. https://doi.org/10.1016/j.cherd.2024.07.056

Yeboah, S., Nunoo, S., Attachie, J., Asihene, W., & Asuamah, E. (2025). Impact and integration techniques of renewable energy sources on smart grid operations: A systematic review. *Scientific African, 29*, e02845. https://doi.org/10.1016/j.sciaf.2025.e02845

Yulianto, E. S., Yuniardi, D., & Harfit, A. R. (2023). System development for enhancing boiler performance: From PID control to adaptive and model predictive control for more effective optimization of temperature, pressure, and level control in boiler system. *International Journal of Science and Technology, 2*(2), 14–23. https://doi.org/10.56127/ijst.v2i2.680

Zahedifar, R., Soleymani Baghshah, M., & Taheri, A. (2025). LLM-controller: Dynamic robot control adaptation using large language models. *Robotics and Autonomous Systems, 186*, 104913. https://doi.org/10.1016/j.robot.2024.104913